HHS Public Access

Author manuscript

Protein Pept Lett. Author manuscript; available in PMC 2023 December 11.

Published in final edited form as:

Protein Pept Lett. 2021 ; 28(9): 963–971. doi:10.2174/0929866528666210806152706.

Nonhuman IAPP Variants Inhibit Human IAPP Aggregation

Alissa Oakes[1], **Kate Menefee**[2], **Arleen Lamba**[1], **Larry M. Palato**[2], **Dillon J. Rinauro**[2], **Angela Tun**[2], **Betssy Jauregui**[2], **Kevin Chang**[2], **Luiza A. Nogaj**[1], **David A. Moffet**[2,*]

[1]Department of Biology, Mount Saint Mary's University, Los Angeles, CA 90049, USA;

[2]Department of Chemistry and Biochemistry, Loyola Marymount University, Los Angeles, CA 90045, USA

Abstract

Aim: To identify naturally occurring variants of IAPP capable of inhibiting the aggregation of human IAPP and protecting living cells from the toxic effects of human IAPP.

Background: The loss of insulin-producing β-cells and the overall progression of type 2 diabetes appears to be linked to the formation of toxic human IAPP (hIAPP, Islet Amyloid Polypeptide, amylin) amyloid in the pancreas. Inhibiting the initial aggregation of hIAPP has the potential to slow, if not stop entirely, the loss of β-cells and halt the progression of the disease.

Objective: To identify and characterize naturally occurring variants of IAPP capable of inhibiting human IAPP aggregation.

Methods: Synthetic human IAPP was incubated with synthetic IAPP variants identified from natural sources under conditions known to promote amyloid-based aggregation. To identify IAPP variants capable of inhibiting human IAPP aggregation, Thioflavin T-binding fluorescence, atomic force microscopy, and cell-rescue assays were performed.

Results: While most IAPP variants showed little to no ability to inhibit human IAPP aggregation, several variants showed some ability to inhibit aggregation, with two variants showing substantial inhibitory potential.

Conclusion: Several naturally occurring IAPP variants capable of inhibiting human IAPP aggregation were identified and characterized.

Keywords

Islet amyloid polypeptide; protein aggregation; amyloid; type 2 diabetes; amylin; pancreas

*Address correspondence to this author at the Department of Chemistry and Biochemistry, Loyola Marymount University, Los Angeles, CA 90045, USA; Tel: 310-338-4400; dmoffet@lmu.edu.

HUMAN AND ANIMAL RIGHTS

No Animals/Humans were used for studies that are the basis of this research.

CONFLICT OF INTEREST

The authors declare no conflict of interest, financial or otherwise.

1. INTRODUCTION

Human Islet Amyloid Polypeptide (hIAPP) is a 37 amino acid hormone co-secreted with insulin from pancreatic β-cells [1, 2]. This peptide hormone circulates through the bloodstream (some blood concentrations are estimated to be as high as 268 pM [3]) and into the brain, where it is credited with slowing gastric emptying and signaling satiety during and after a meal [4, 5]. Patients with type 1 diabetes, who no longer possess the ability to produce insulin or hIAPP, often take hIAPP mimetic supplements (pramlintide) with positive benefits that include satiety after a meal, a decrease in the amount of insulin needed to control blood-sugar concentrations and an average weight loss of about 2 kg [4]. The complete role of hIAPP within the body remains to be determined, but it seems to be an important part of metabolic glucose control.

While hIAPP appears to be a beneficial peptide hormone for controlling appetite, it does seem to play a role in the progression of type 2 diabetes [6–8]. hIAPP is one of the most aggregation-prone amyloidogenic peptides known [9]. This peptide is known to self-assemble into toxic amyloid extracellularly within the pancreas, where it is believed to cause the loss of pancreatic tissue in patients with type 2 diabetes [4, 10–14]. Some reports claim that 95% of type 2 diabetes patients have deposits of hIAPP amyloid within their pancreas [10–12].

The IAPP hormone is found throughout the animal kingdom. However, its peptide sequence is not entirely conserved across species. IAPP amyloidogenicity appears to be highly sequence-dependent, with some variants (such as hIAPP) extremely amyloidogenic and other variants (such as rat) highly resistant to aggregation and amyloid formation [15]. Recent work indicates that those species expressing amyloidogenic variants of IAPP tend to be more prone to developing diabetes whereas those species expressing non-amyloidogenic variants of IAPP tend to be resistant to developing diabetes [16, 17]. For example, rats, mice, pigs, bears and cows express variants of IAPP that are non-amyloidogenic. None of these species are known to spontaneously develop type 2 diabetes-like conditions [18]. However, organisms such as humans, cats, monkeys, dogs, chickens, and raccoons express amyloidogenic IAPP variants and each of these species is known to have the potential to develop diabetic symptoms [18].

If hIAPP aggregation leads to loss of pancreatic mass and the progression of type 2 diabetes, inhibitors of hIAPP aggregation have the potential to slow, if not halt altogether, the progression of the disease [19]. Here, we identify and characterize naturally occurring IAPP peptide variants capable of inhibiting the formation of toxic hIAPP amyloid.

2. MATERIALS AND METHODS

2.1. Preparing Disaggregated IAPP

Synthetic human IAPP was from Lifetein (Somerset, NJ) and >95% pure. Initial studies of synthetic animal IAPP peptides were from WatsonBio Sciences (Houston, TX) with purities between 80–96%. To confirm results, high purity IAPP variants were purchased from both Watson Bio Sciences (Houston, TX) and Lifetein (Somerset, NJ) (Table 1). All

synthetic IAPP variants were dissolved in hexafluorisopropanol (HFIP, Sigma-Aldrich) to 0.125 mg/mL and placed in a sonicating water bath for 10 minutes and immediately stored at −80°C.

2.2. Thioflavin T Binding Assays

hIAPP alone, or hIAPP mixed with an animal IAPP variant, was pipetted into a glass tube and the HFIP was removed under speed-vacuum. The resulting peptide sample was dissolved in 20 mM tris buffer pH 7.40. The final in-solution concentrations of hIAPP and each animal IAPP are indicated for each assay. Aggregation was initiated by incubating samples at 37°C with shaking (200 rpm). At indicated time points, 17 μL aliquot of each sample was mixed with 663 μL of 50.0 μM thioflavin T in 20 mM Tris buffer pH 7.40. Thioflavin T fluorescence emission was recorded (Ex_{450nm}) using a Hitachi F-7000 fluorescence spectrophotometer.

2.3. Atomic Force Microscopy

Samples were prepared as described above. Human IAPP with or without animal IAPP variants were incubated with shaking at 37°C for 40 minutes. After this incubation, 17 μL of each sample was deposited onto freshly cleaved mica. Samples were incubated for 5 minutes at room temperature before washing with 200 μL sterile water. After drying, the samples were scanned using an MFP-3D atomic force microscope (Asylum Research) set on A/C mode and a 240 μm silicon cantilever (Catalog #AC240TS, Olympus). Images shown are the raw data with no flattening.

2.4. Cell Viability Assay

MTT calorimetric assay measuring the conversion of yellow tetrazolium salt into purple formazan crystal catalyzed by a mitochondrial reductase was used. Cell viability studies were performed using RIN-m cells (ATCC, CRL-2057) [20]. An equal number of RIN-m cells were plated in triplicate and incubated overnight in 96-well plates. The next day, fresh RPMI-1640 with phenol red supplemented with 10% FBS was added to cells. Hexafluoroisopropanol (HFIP) was removed from each individual human and animal IAPP using a centrivap concentrator (LabOnco). All IAPP samples were re-suspended in RPMI-1640 with 10% FBS. To ensure even re-suspension, each resulting IAPP-containing vial was scraped with a pipette tip six times and vortexed (Vortex Genie Mixer) for 30 seconds. The whole process, from drying each IAPP to adding each IAPP to the cells was uniform to ensure each sample was incubated for an equal amount of time with each IAPP variant. IAPPs were added to cells at various specified concentrations and incubated for 48 h at 37°C. Post-incubation, the media in each well were replaced by fresh DMEM/F-12 without phenol red. MTT (3-(4,5-dimethyl-2-thiazolyl)-2,5-diphenyl-tetrazolium bromide) was added into each well and incubated at 37°C for 2h. Formazan crystals, formed on the bottom of the wells, were re-suspended in solubilization buffer (20% SDS and 50% dimethylformamide). The absorbance in each well was taken at 570 nm using a Multiskan FC Microplate Photometer (Thermo Fisher Scientific). Media and FBS were obtained from ATCC. All incubations took place in a water-jacketed incubator in 5% carbon dioxide at 37°C (Shell Lab).

2.5. Cell Cytotoxicity Assay

LDH cytotoxicity assay was used to measure the amount of LDH released into the media upon membrane damage. IAPP variants were added to RIN-m cells as described above and incubated at 37°C for 48 hours. Two extra wells of cells were prepared to determine spontaneous and maximum LDH release controls. Post-incubation, Pierce LDH cytotoxicity assay kit (Thermo Fisher) was used to develop each sample according to the manufacturer's instructions. Briefly, 10 μL of water and lysis buffer were added to appropriate wells and incubated for 45 minutes in the cell culture incubator. 50 μL of each sample was transferred to a new 96-well plate and mixed with 50 μL of the reaction mixture. The samples were incubated for 30 minutes at room temperature in the dark before the addition of 50 μL of stop solution. Absorbance was measured at 450 nm and 620 nm using a Thermo Scientific Multiskan FC plate reader (Fisher Scientific). Percent cytotoxicity was calculated using the equation provided by the manufacturer.

2.6. Cell Imaging

Cell morphology was examined using Motic AE31E Microscope solutions with Moticam 3.0 MP camera.

3. RESULTS

The amino acid sequence of human IAPP (hIAPP) is compared to the amino acid sequences of the animal IAPP variants investigated in this study (Figure 1). The animal variants identified in this work as showing potential for inhibiting hIAPP aggregation are listed at the top of the figure, while those variants lacking inhibitory potential are listed at the bottom. Only amino acids that differ from the sequence of hIAPP are indicated in the figure.

To identify variants having inhibitory potential against hIAPP aggregation, each variant was mixed with hIAPP (2:1 molar ratio of animal variant to hIAPP) and incubated under conditions known to promote hIAPP aggregation and fibril formation. Over 40 minutes, these samples were monitored for their ability to bind thioflavin T (Figure 2) and their ability to form fibrils as identified with atomic force microscopy (AFM) (Figures 3 and 4). Thioflavin T binding is a common technique for identifying amyloid formation in real-time [21]. Because hIAPP is known to bind thioflavin T during aggregation and amyloid formation, the technique proves to be a simple method for identifying substances with amyloid-inhibiting potential. Unfortunately, thioflavin T binding is known to yield false positives when, for instance, the inhibitor does not prevent amyloid formation, but rather prevents thioflavin T from binding to the amyloid. From previous work performed by us and others, thioflavin T does not bind well to all variants of IAPP, and could not be relied on solely to identify inhibitory IAPP variants [18, 22].

AFM was used to test the amyloid-inhibitory potential of each variant directly. hIAPP, under these amyloid-forming conditions, forms high-density plaques of fibrils when deposited onto mica and scanned *via* AFM (Figures 3 and 4) [23, 24]. Likewise, many of the animal IAPP variants are known to form fibrils by themselves (without hIAPP present) and yield amyloid-plaques when scanned *via* AFM [18]. In these mixing studies, cow, degu dolphin,

guinea pig, horse, pig, rat, and sheep IAPP variants either had no effect on hIAPP fibril formation or formed fibrils with hIAPP (Figure 3). Five IAPP variants were found to show at least modest ability to inhibit hIAPP fibril formation (Figure 4). Chicken, cat, polar bear, raccoon, and seal all showed significant ability to prevent fiber formation. Interestingly, all of these variants except polar bear are known to aggregate and form fibrils themselves (without hIAPP) under these (or similar) conditions [16, 18].

To identify the strongest *in vitro* inhibitors of hIAPP aggregation, animal variants were diluted while holding the concentration of hIAPP constant at 37 μM. Cat, polar bear, and seal appeared to lose inhibitory capability when mixed with hIAPP at a 1:1 molar ratio (data not shown). Chicken IAPP continued to show some inhibition (some fibers were identified, but vastly fewer than hIAPP alone). However, raccoon IAPP was the strongest *in vitro* inhibitor of hIAPP aggregation. Raccoon IAPP continued to show inhibitory efficacy against 37 μM hIAPP at 18.5 μM (Figure 5).

Several assays were performed to identify the peptide variants with the greatest ability to rescue cells from the toxic effects of hIAPP. The MTT assay was used to measure the effect of each IAPP variant (human and non-human) on the viability of RIN-m cells. RIN-m cells alone were set as one hundred percent viable and were used as a positive control (Figure 6, black bar). Human IAPP and each individual animal IAPP variant were added to cells separately to determine their effect on cell viability relative to cells alone (Figure 6, blue bars). Animal IAPPs were mixed with hIAPP at a 1:1 molar ratio (Figure 6, red bars) and their combined effects on RIN-m cell viability were determined. hIAPP was consistently toxic to the cells. A 12.8 μM hIAPP concentration resulted in a decrease in cell viability by 45+/−5%. IAPPs from raccoon and cat resulted in an average decrease of cell viability of about 25%, while IAPPs from seal and polar bear decreased cell viability by 20%. Chicken IAPP was not as toxic to the cells with an average of 10% decrease in cell viability. Rat IAPP did not show a significant effect on cells. Mixing raccoon IAPP or chicken IAPP with hIAPP consistently rescued cells to 72% and 76% viability, respectively. Both cat and seal IAPPs were capable of cell rescue from the toxic effect of hIAPP but those results were not significant. Both polar bear IAPP and rat IAPP were unable to rescue cells from the toxic effects of hIAPP (Figure 6, red bars).

The LDH cytotoxicity assay was used to measure the amount of LDH released into the cell culture media as a result of damage to the cellular plasma membrane (Figure 7). Cells alone showed no cytotoxicity, while the addition of hIAPP to RIN-m cells increased the release of LDH into the media. The addition of raccoon, chicken, cat, seal, and polar bear IAPPs to the cells showed some damage to the plasma membrane of the cells, but much less compared to hIAPP. Rat IAPP on its own had very little effect on the cellular plasma membrane. Mixing hIAPP with raccoon, chicken, cat, seal, or polar bear IAPP decreased the toxicity of hIAPP and reduced the amount of damage to the plasma membrane. The addition of rat IAPP to hIAPP increased the amount of cytotoxicity in the cell.

The morphology of RIN-m cells changed upon incubation with toxic hIAPP. RIN-m cell morphology was examined when incubated with each individual IAPP as well as when each non-human IAPP was mixed with hIAPP (Figure 8). RIN-m cells alone showed

epithelial-like structure and grew in distinct patches firmly attached to the plate surface. The addition of hIAPP resulted in changes in cellular shape, formation of granular nuclear structures, and detachment of numerous cells from the plate surface. When incubated with RIN-m cells individually (in the absence of hIAPP), raccoon, chicken, and rat IAPP did not cause significant changes to RIN-m morphology. Incubation of cat, seal, or polar bear IAPP with RIN-M cells (in the absence of hIAPP) showed some rounding of cells and detaching from the plate. Mixing of raccoon IAPP or chicken IAPP with hIAPP resulted in cells that maintained their epithelial shape and remained attached to the plate. Mixing of cat IAPP or seal IAPP with hIAPP resulted in cells looking better than cells incubated with hIAPP alone, but the resulting cellular morphology was different from cells alone (cells remained attached to the plate, but some granular nuclear structures could be seen). Polar bear IAPP mixed with hIAPP resulted in patches of rounded cells. Mixing of rat IAPP with hIAPP resulted in many cells with a round shape and detached from the plate.

4. DISCUSSION

Naturally occurring peptides, such as rat IAPP, have been previously identified as modest inhibitors of hIAPP aggregation [25, 26]. Rat IAPP, however, does not independently aggregate, form fibrils, or show toxicity to living cells [27–29]. In this report, we identified several hIAPP amyloid inhibitors from a collection of naturally occurring variants that form amyloid, produce fibrils, and are toxic to cells themselves (independently of hIAPP). IAPP from cat, chicken, raccoon, and seal are all known to form amyloid fibrils [18]. Under these experimental conditions, mixing fibril-forming hIAPP with any of these fibril-forming IAPP variants led to a cessation of fibril-formation and reduced levels of toxicity due to hIAPP.

The two IAPP variants showing the strongest inhibitory potential *in vitro*, chicken and raccoon, were also the two variants showing the greatest ability to rescue living cells from toxic hIAPP. While seal, polar bear, and cat IAPP showed *in vitro* that they could inhibit hIAPP aggregation at 2 to 1 molar ratios, they showed little ability to rescue cells from hIAPP at 1 to 1 molar ratios.

It is unlikely that a single amino acid substitution between hIAPP and an animal variant is the sole driving force behind the inhibition of aggregation. When comparing the amino acid sequences of hIAPP and the inhibitory animal IAPP variants, three amino acids are mostly conserved among the inhibitory peptides, H18R, F23L, and S29P (Figure 1). Yet, these three conserved positions exist also in many of the non-inhibitory peptides. All thirteen animal variants described here have the S29P exchange (five inhibit hIAPP aggregation and eight show no effect), making it unlikely that this is the driving force behind the inhibition of hIAPP. Likewise, ten of the thirteen variants described here have the F23L substitution (three inhibit hIAPP aggregation and seven show no effect) and ten out of thirteen possess the H18R substitution (five inhibit hIAPP aggregation and five show no effect).

The results suggest that these three substitutions (H18R, F23L, and S29P) are important for inhibition of hIAPP aggregation, but that another factor is also likely to be necessary. When comparing the inhibitor peptides from non-inhibitors, what stands out is the number of amino acid substitutions in the H18-S28 region of the peptide. This region has long been

suggested as being important for hIAPP self-assembly [15, 30–32]. Likewise, this region has led to the identification of short peptide inhibitors of hIAPP aggregation that specifically target the 20–29 region of hIAPP [33–39]. In this study, the majority of peptides that inhibit hIAPP aggregation have the three substitutions described above (H18R, F23L, and S29P) and have few additional substitutions in the H18-S28 region. Whereas, the non-inhibitory peptides seemed to either have a preponderance of substitutions in the H18-S28 region and/or lacked the H18R, F23L, and S29P substitutions. It is likely that the H18-S28 region is necessary for the inhibitor peptides to interact with hIAPP, while the H18R, F23L, and S29P substitutions (or some combination thereof) are necessary for the observed inhibitory activity.

Inhibition of amyloid formation by naturally occurring homologs is not limited to IAPP. Previous work has identified homologs of alpha-Synuclein, the amyloid protein believed to be directly involved in the progression of Parkinson's Disease, as inhibitors of amyloid and fibril formation [40–42]. Both beta- and gamma- synculeins have been shown to be capable of inhibiting alpha-synuclein aggregation and fiber formation [43].

CONCLUSION

While the root cause of type 2 diabetes remains to be determined, the cytotoxicity of hIAPP and concomitant loss of β-cell mass seem to participate in the progression of the disease [44, 45]. Inhibiting the formation of hIAPP toxic species could slow, if not stop altogether, the progression of the disease. Because hIAPP is excreted extracellularly, small peptides, such as hIAPP analogs or animal IAPP variants, could be potential therapeutic agents for inhibiting hIAPP amyloidogenicity and protecting cellular viability. Several naturally occurring IAPP variants are identified and characterized for their ability to inhibit hIAPP aggregation and cellular toxicity.

ACKNOWLEDGEMENTS

The authors wish to thank the LMU Seaver College of Science and Engineering, the LMU Honors program, and the MSMU Department of Biology for support of this work.

FUNDING

This work was supported by the National Institutes of Health, USA under Grant 1R15DK112172-02.

LIST OF ABBREVIATIONS

IAPP	Islet Amyloid Polypeptide
hIAPP	human IAPP
ThT	Thioflavin T
HFIP	Hexafluoroisopropanol
AFM	Atomic Force Microscope
MTT	1-(4,5-Dimethylthiazol-2-yl)-3,5-diphenylformazan

REFERENCES

[1]. Montane J; Klimek-Abercrombie A; Potter KJ; Westwell-Roper C; Bruce Verchere C Metabolic stress, IAPP and islet amyloid. Diabetes Obes. Metab, 2012, 14(Suppl. 3), 68–77. 10.1111/j.1463-1326.2012.01657.x [PubMed: 22928566]

[2]. Asthana S; Mallick B; Alexandrescu AT; Jha S IAPP in type II diabetes: Basic research on structure, molecular interactions, and disease mechanisms suggests potential intervention strategies. Biochim. Biophys. Acta, 2018, 1860(9), 1765–1782. 10.1016/j.bbamem.2018.02.020

[3]. Paulsson JF; Ludvigsson J; Carlsson A High plasma levels of islet amyloid polypeptide in young with new-onset of type 1 diabetes mellitus. PLoS One, 2014, 9(3), e93053. 10.1371/journal.pone.0093053 [PubMed: 24671002]

[4]. Ling W; Huang YM; Qiao YC; Zhang XX; Zhao HL Human amylin: From pathology to physiology and pharmacology. Curr. Protein Pept. Sci, 2019, 20(9), 944–957. 10.2174/1389203720666190328111833 [PubMed: 30919775]

[5]. Cao P; Abedini A; Raleigh DP Aggregation of islet amyloid polypeptide: from physical chemistry to cell biology. Curr. Opin. Struct. Biol, 2013, 23(1), 82–9. 10.1016/j.sbi.2012.11.003 [PubMed: 23266002]

[6]. Bucciantini M; Giannoni E; Chiti F Inherent toxicity of aggregates implies a common mechanism for protein misfolding diseases. Nature, 2002, 416(6880), 507–511. 10.1038/416507a [PubMed: 11932737]

[7]. Chiti F; Dobson CM Protein misfolding, functional amyloid, and human disease. Annu. Rev. Biochem, 2006, 75, 333–366. 10.1146/annurev.biochem.75.101304.123901 [PubMed: 16756495]

[8]. Murphy RM; Kendrick BS Protein misfolding and aggregation. Biotechnol. Prog, 2007, 23(3), 548–552. 10.1021/bp060374h [PubMed: 17425329]

[9]. Abedini A; Schmidt AM Mechanisms of islet amyloidosis toxicity in type 2 diabetes. FEBS Lett, 2013, 587(8), 1119–1127. 10.1016/j.febslet.2013.01.017 [PubMed: 23337872]

[10]. Apostolidou M; Jayasinghe SA; Langen R Structure of alpha-helical membrane-bound human islet amyloid polypeptide and its implications for membrane-mediated misfolding. J. Biol. Chem, 2008, 283(25), 17205–17210. 10.1074/jbc.M801383200 [PubMed: 18442979]

[11]. Hull RL; Westermark GT; Westermark P; Kahn SE Islet amyloid: a critical entity in the pathogenesis of type 2 diabetes. J. Clin. Endocrinol. Metab, 2004, 89(8), 3629–3643. 10.1210/jc.2004-0405 [PubMed: 15292279]

[12]. Kahn SE; Andrikopoulos S; Verchere CB Islet amyloid: a long-recognized but underappreciated pathological feature of type 2 diabetes. Diabetes, 1999, 48(2), 241–253. 10.2337/diabetes.48.2.241 [PubMed: 10334297]

[13]. Patel HR; Pithadia AS; Brender JR; Fierk CA; Ramamoorthy A In search of aggregation pathways of IAPP and other amyloidogenic proteins: finding answers through NMR spectroscopy. J. Phys. Chem. Lett, 2014, 5(11), 1864–1870. 10.1021/jz5001775 [PubMed: 26273866]

[14]. Moore SJ; Sonar K; Bharadwaj P Characterisation of the structure and oligomerisation of islet amyloid polypeptides (IAPP): a review of molecular dynamics simulation studies. Molecules, 2018, 23(9), 2142. 10.3390/molecules23092142 [PubMed: 30149632]

[15]. Westermark P; Engstrom U; Johnson KH Islet amyloid polypeptide: pinpointing amino acid residues linked to amyloid fibril formation. Proc. Natl. Acad. Sci. USA, 1990, 87(13), 5036–5040. 10.1073/pnas.87.13.5036 [PubMed: 2195544]

[16]. Fortin JS; Benoit-Biancamano MO Wildlife sequences of islet amyloid polypeptide (IAPP) identify critical species variants for fibrillization. Amyloid, 2015, 22(3), 194–202. 10.3109/13506129.2015.1070824 [PubMed: 26300107]

[17]. Betsholtz C; Christmanson L; Engstrom U; Rorsman F; Jordan K; O'Brien TD; Murtaugh M; Johnson KH; Westermark P Structure of cat islet amyloid polypeptide and identification of amino-acid-residues of potential significance for islet amyloid formation. Diabetes, 1990, 39(1), 118–122. 10.2337/diacare.39.1.118 [PubMed: 2210054]

[18]. Palato LM; Pilcher S; Oakes A; Lamba A; Torres J; Ledesma Monjaraz LI; Munoz C; Njoo E; Rinauro DJ; Menefee KA; Tun A; Jauregui BL; Shapiro S; Nossiff OH; Olivares E; Chang K;

Nguyen V; Nogaj LA; Moffet DA Amyloidogenicity of naturally occurring full-length animal IAPP variants. J. Pept. Sci, 2019, 25(8), e3199. 10.1002/psc.3199 [PubMed: 31231935]

[19]. Denroche HC; Verchere CB IAPP and type 1 diabetes: implications for immunity, metabolism and islet transplants. J. Mol. Endocrinol, 2018, 60(2), R57–R75. 10.1530/JME-17-0138 [PubMed: 29378867]

[20]. Suzuki S; Murakami M; Abe S; Satoh Y; Shintani S; Ishizuka J; Suzuki K; Thompson JC; Toyota T The effects of amylin on insulin secretion from Rin m5F cells and glycogen synthesis and lipogenesis in rat primary cultured hepatocytes. Diabetes Res. Clin. Pract, 1992, 15(1), 77–84. 10.1016/0168-8227(92)90071-X [PubMed: 1311671]

[21]. Higham CE; Jaikaran ET; Fraser PE; Gross M; Clark A Preparation of synthetic human islet amyloid polypeptide (IAPP) in a stable conformation to enable study of conversion to amyloid-like fibrils. FEBS Lett, 2000, 470(1), 55–60. 10.1016/S0014-5793(00)01287-4 [PubMed: 10722845]

[22]. Wong AG; Wu C; Hannaberry E Analysis of the amyloidogenic potential of pufferfish (*Takifugu rubripes*) islet amyloid polypeptide highlights the limitations of thioflavin-t assays and the difficulties in defining amyloidogenicity. Biochemistry, 2016, 55(3), 510–518. 10.1021/acs.biochem.5b01107 [PubMed: 26694855]

[23]. Kayed R; Bernhagen J; Greenfield N; Sweimeh K; Brunner H; Voelter W; Kapurniotu A Conformational transitions of islet amyloid polypeptide (IAPP) in amyloid formation *in vitro*. J. Mol. Biol, 1999, 287(4), 781–796. 10.1006/jmbi.1999.2646 [PubMed: 10191146]

[24]. Watanabe-Nakayama T; Sahoo BR; Ramamoorthy A High-speed atomic force microscopy reveals the structural dynamics of the amyloid-beta and amylin aggregation pathways. Int. J. Mol. Sci, 2020, 21(12), 4287. [PubMed: 32560229]

[25]. Berhanu WM; Hansmann UH Inter-species cross-seeding: stability and assembly of rat-human amylin aggregates. PLoS One, 2014, 9(5), e97051. [PubMed: 24810618]

[26]. Middleton CT; Marek P; Cao P Two-dimensional infrared spectroscopy reveals the complex behaviour of an amyloid fibril inhibitor. Nat. Chem, 2012, 5(4), 355–360. 10.1038/nchem.1293

[27]. Zhang M; Hu R; Liang G; Chang Y; Sun Y; Peng Z; Zheng J Structural and energetic insight into the cross-seeding amyloid assemblies of human IAPP and rat IAPP. J. Phys. Chem. B, 2014, 118(25), 7026–7036. 10.1021/jp5022246 [PubMed: 24892388]

[28]. Liang G; Zhao J; Yu X; Zheng J Comparative molecular dynamics study of human islet amyloid polypeptide (IAPP) and rat IAPP oligomers. Biochemistry, 2013, 52(6), 1089–1100. 10.1021/bi301525e [PubMed: 23331123]

[29]. Mazzaglia A; Micali N; Scolaro LM; Attanasio F; Magrí A; Pappalardo G; Villari V Aggregation properties of the peptide fragments derived from the 17–29 region of the human and rat IAPP: a comparative study with two PEG-conjugated variants of the human sequence. J. Phys. Chem. B, 2010, 114(2), 705–713. 10.1021/jp908436s [PubMed: 20039665]

[30]. Fox A; Snollaerts T; Casanova CE Selection for nonamyloidogenic mutants of islet amyloid polypeptide (IAPP) identifies an extended region for amyloidogenicity. Biochemistry, 2010, 49(36), 7783–7789. [PubMed: 20698575]

[31]. Gazit E Mechanisms of amyloid fibril self-assembly and inhibition. FEBS J, 2005, 272(23), 5971–5978. 10.1111/j.1742-4658.2005.05022.x [PubMed: 16302962]

[32]. Nanga RP; Brender JR; Xu J; Veglia G; Ramamoorthy A Structures of rat and human islet amyloid polypeptide IAPP(1–19) in micelles by NMR spectroscopy. Biochemistry, 2008, 47(48), 12689–12697. 10.1021/bi8014357 [PubMed: 18989932]

[33]. Abedini A; Raleigh DP Destabilization of human IAPP amyloid fibrils by proline mutations outside of the putative amyloidogenic domain: is there a critical amyloidogenic domain in human IAPP? J Mol Biol, 2006, 355(2), 274–281. [PubMed: 16303136]

[34]. Marek P; Abedini A; Song BB Aromatic interactions are not required for amyloid fibril formation by islet amyloid polypeptide but do influence the rate of fibril formation and fibril morphology. Biochemistry, 2007, 4611, 3255–3261. 10.1021/bi0621967

[35]. Abedini A; Meng FL; Raleigh DP A single-point mutation converts the highly amyloidogenic human islet amyloid polypeptide into a potent fibrillization inhibitor. J. Am. Chem. Soc, 2007, 129(37), 11300. 10.1021/ja072157y [PubMed: 17722920]

[36]. Abedini A; Raleigh DP The role of His-18 in amyloid formation by human islet amyloid polypeptide. Biochemistry, 2005, 44(49), 16284–16291. 10.1021/bi051432v [PubMed: 16331989]

[37]. Koo BW; Hebda JA; Miranker AD Amide inequivalence in the fibrillar assembly of islet amyloid polypeptide. Protein Eng. Des. Sel, 2008, 21(3), 147–154. 10.1093/protein/gzm076 [PubMed: 18299291]

[38]. Scrocchi LA; Chen Y; Waschuk S Design of peptide-based inhibitors of human islet amyloid polypeptide fibrillogenesis. J. Mol. Biol, 2002, 318(3), 697–706. 10.1016/S0022-2836(02)00164-X [PubMed: 12054816]

[39]. Tracz SM; Abedini A; Driscoll M; Raleigh DP Role of aromatic interactions in amyloid formation by peptides derived from human Amylin. Biochemistry, 2004, 43(50), 15901–15908. 10.1021/bi048812l [PubMed: 15595845]

[40]. Park JY; Lansbury PT Jr. Beta-synuclein inhibits formation of alpha-synuclein protofibrils: A possible therapeutic strategy against Parkinson's disease. Biochemistry, 2003, 42(13), 3696–3700. 10.1021/bi020604a [PubMed: 12667059]

[41]. Kessler JC; Rochet JC; Lansbury PT Jr, The N-terminal repeat domain of alpha-synuclein inhibits beta-sheet and amyloid fibril formation. Biochemistry, 2003, 42(3), 672–678. 10.1021/bi020429y [PubMed: 12534279]

[42]. Rochet JC; Conway KA; Lansbury PT Jr, Inhibition of fibrillization and accumulation of prefibrillar oligomers in mixtures of human and mouse alpha-synuclein. Biochemistry, 2000, 39(35), 10619–10626. 10.1021/bi001315u [PubMed: 10978144]

[43]. Uversky VN; Li J; Souillac P; Millett IS; Doniach S; Jakes R; Goedert M; Fink AL Biophysical properties of the synucleins and their propensities to fibrillate: inhibition of alpha-synuclein assembly by beta- and gamma-synucleins. J. Biol. Chem, 2002, 277(14), 11970–11978. 10.1074/jbc.M109541200 [PubMed: 11812782]

[44]. Kanatsuka A; Kou S; Makino H IAPP/amylin and beta-cell failure: implication of the risk factors of type 2 diabetes. Diabetol Int, 2018, 9(3), 143–157. 10.1007/s13340-018-0347-1 [PubMed: 30603362]

[45]. Kim J; Park K; Kim MJ An autophagy enhancer ameliorates diabetes of human IAPP-transgenic mice through clearance of amyloidogenic oligomer. Nat Commun, 2021, 12(1), 183. 10.1038/s41467-020-20454-z [PubMed: 33420039]

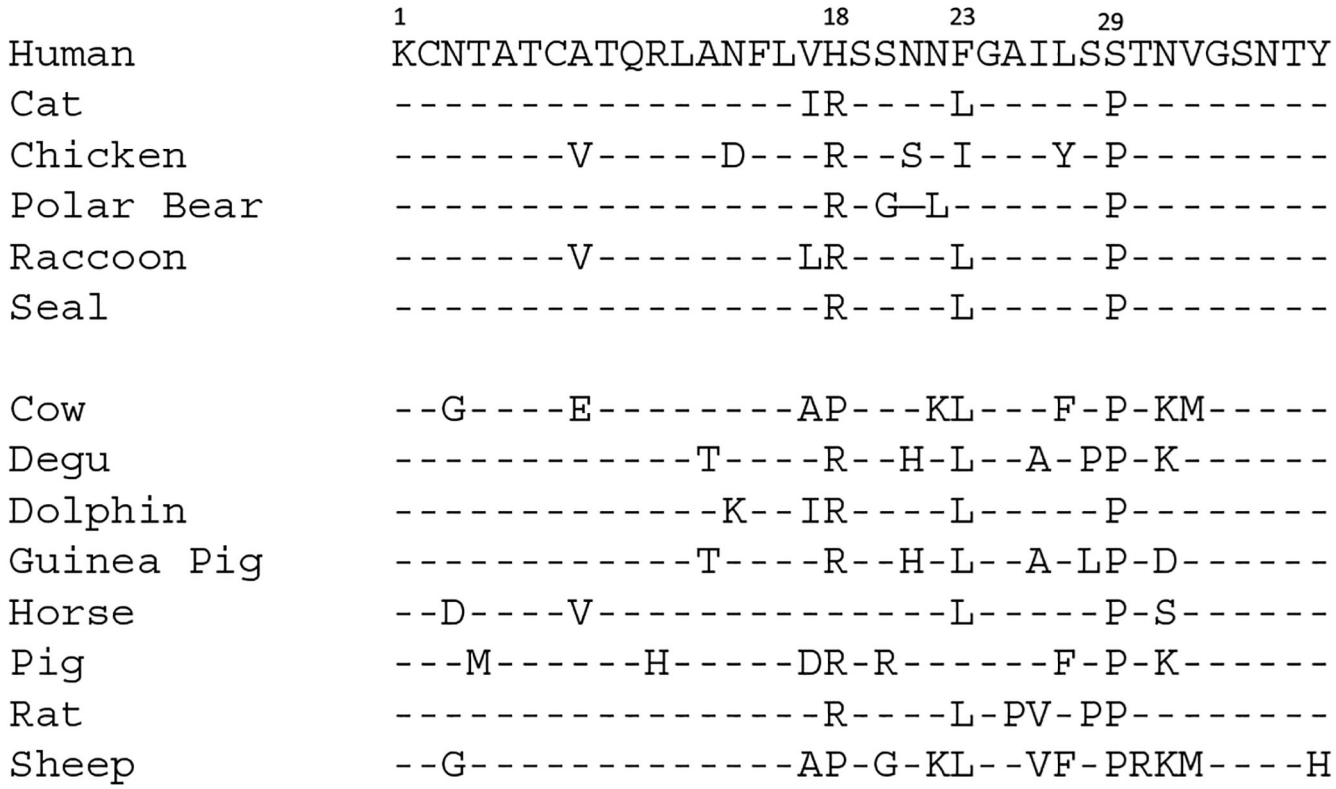

Figure 1.

Sequence comparison between human IAPP and animal IAPP variants in this study. Only amino acids that differ from the sequence of hIAPP are indicated. IAPP variants found to inhibit hIAPP aggregation are indicated in the top half of the figure, with variants showing no ability to inhibit hIAPP aggregation listed in the bottom half of the figure.

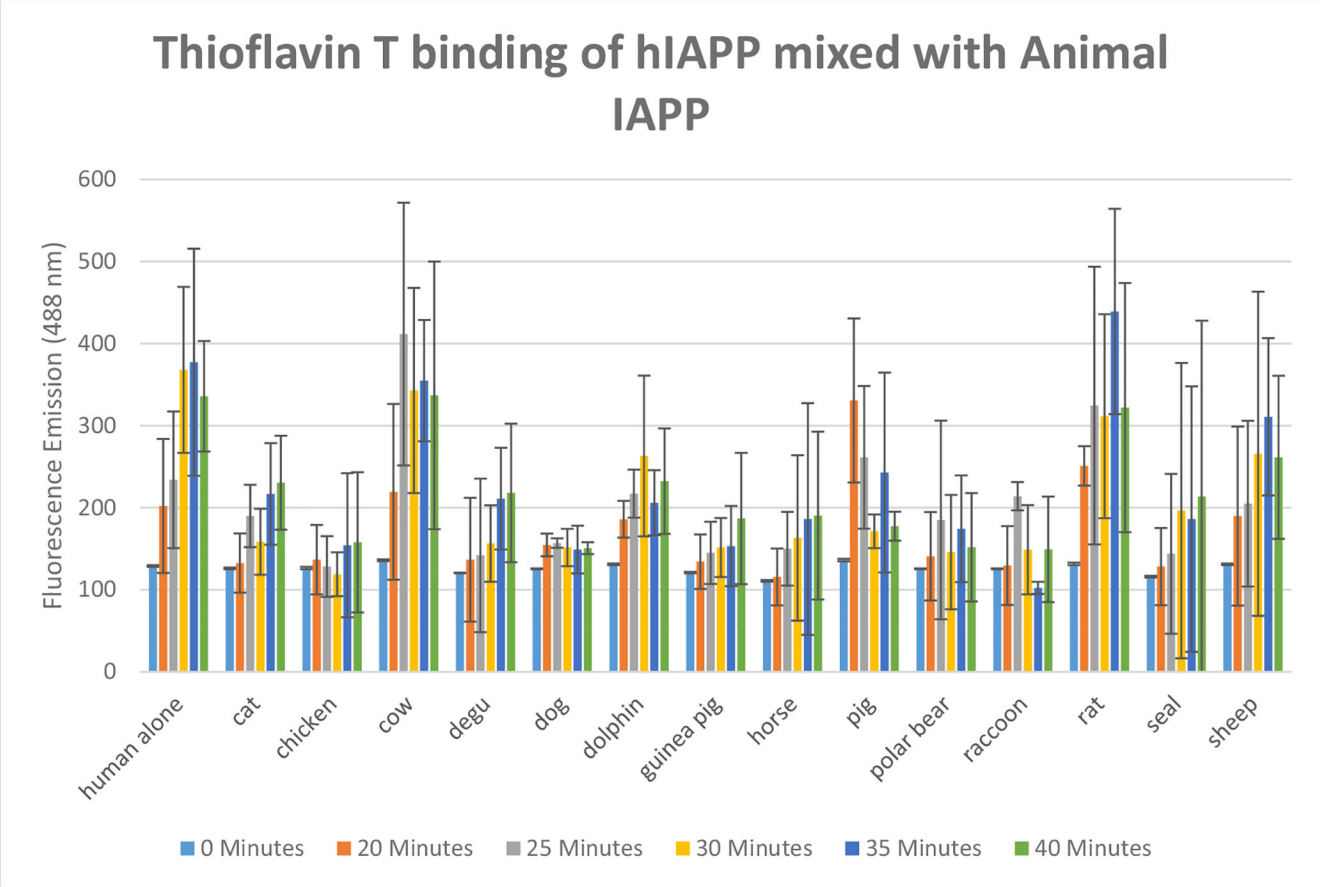

Figure 2.

37 μM Human IAPP mixed with 75 μM of each indicated animal IAPP. Samples were incubated at 37°C for 40 minutes with shaking. Fluorescence at 488 nm was recorded at the indicated time points. The average of at least three trials is shown with error bars indicating the standard deviation among trials.

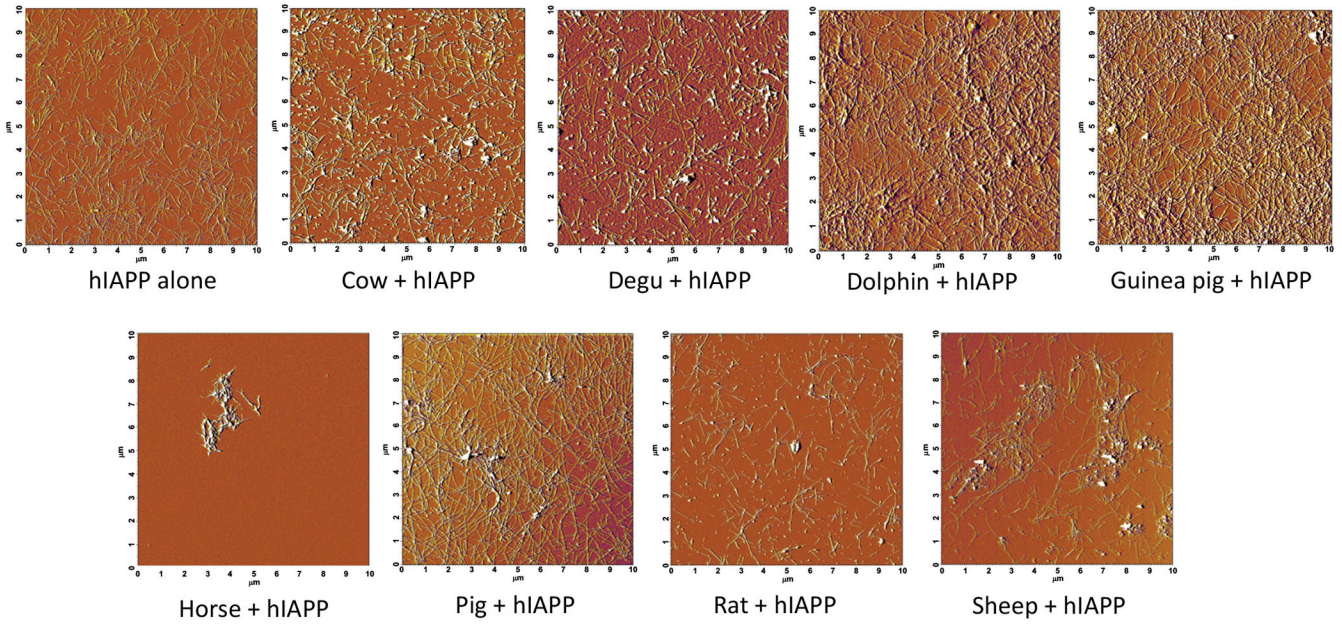

Figure 3.

IAPP variants showing no inhibition of hIAPP aggregation. 37 uM Human IAPP mixed with 75 uM of each animal IAPP. Samples were incubated at 37 degrees C for 40 minutes with shaking. All scans are shown as 10 μM × 10 μM.

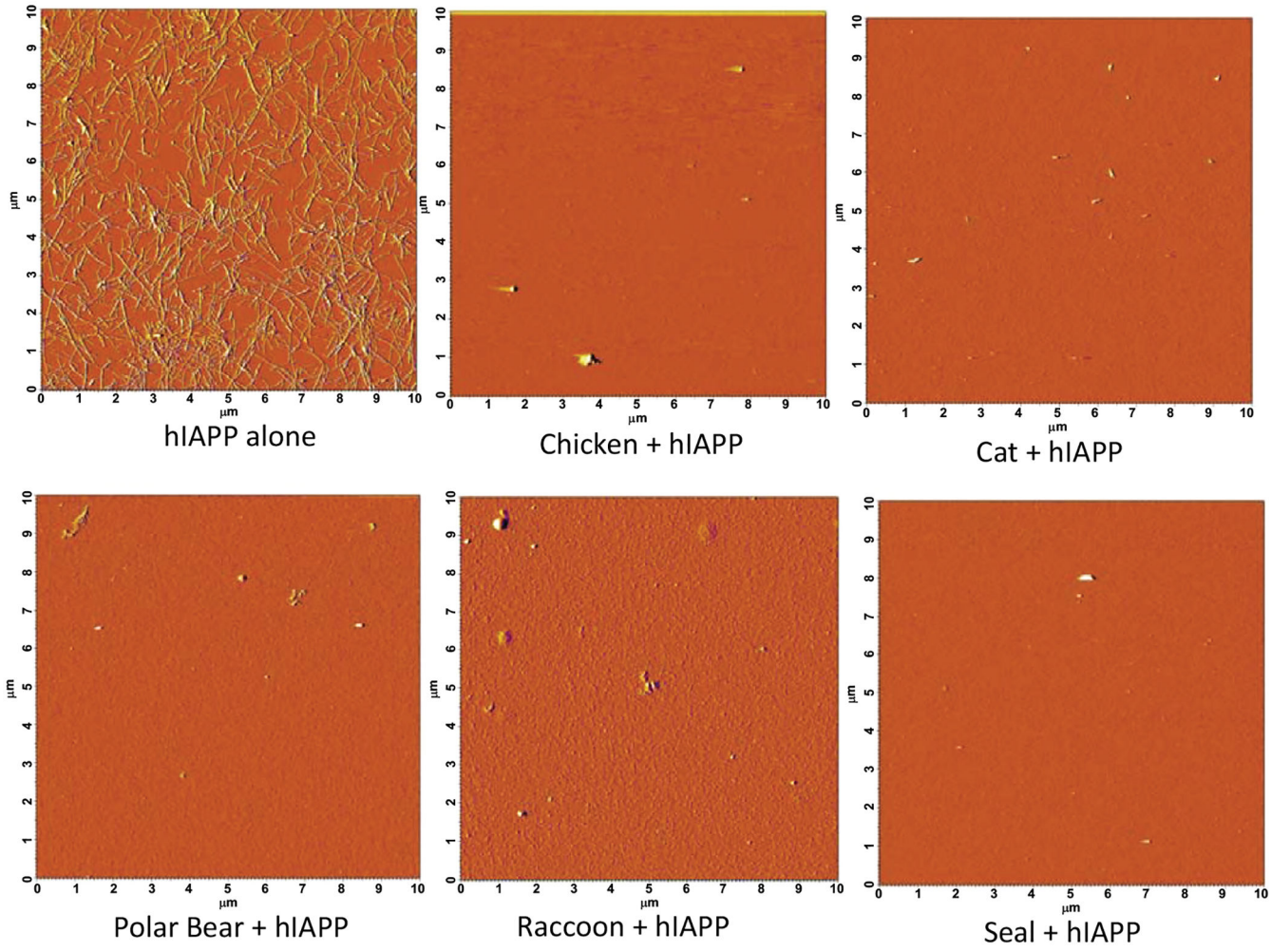

Figure 4.

IAPP variants showing inhibitory potential against hIAPP aggregation. 37 uM Human IAPP mixed with 75 uM of each animal IAPP. Samples were incubated at 37 degrees C for 40 minutes with shaking. All scans are shown as 10 µM x 10 µM.

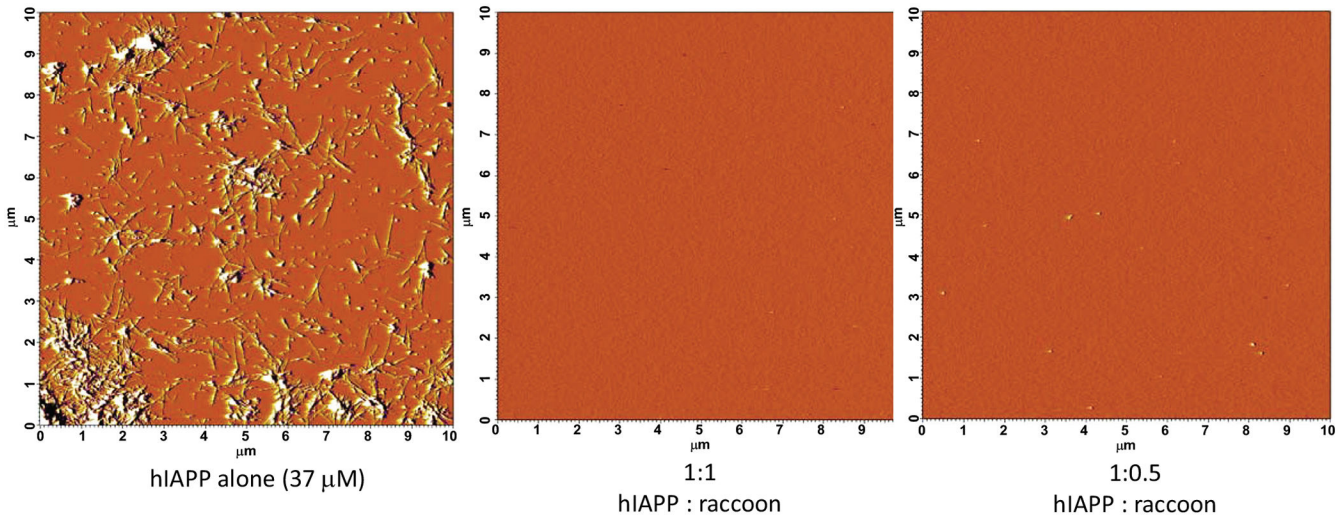

Figure 5.

AFM images of hIAPP with dilutions of raccoon IAPP. Inhibition of hIAPP aggregation with diluted concentrations of raccoon of raccoon IAPP. All samples contained 37 μM hIAPP. 1:1 sample contained 37 μM hIAPP mixed with 37 μM raccoon IAPP. 1:0.5 sample contained 37 μM hIAPP mixed with 18.5 μM raccoon IAPP. Samples were mixed at 37°C for 40 minutes with shaking at 200 rpm prior to depositing onto freshly cleaved mica.

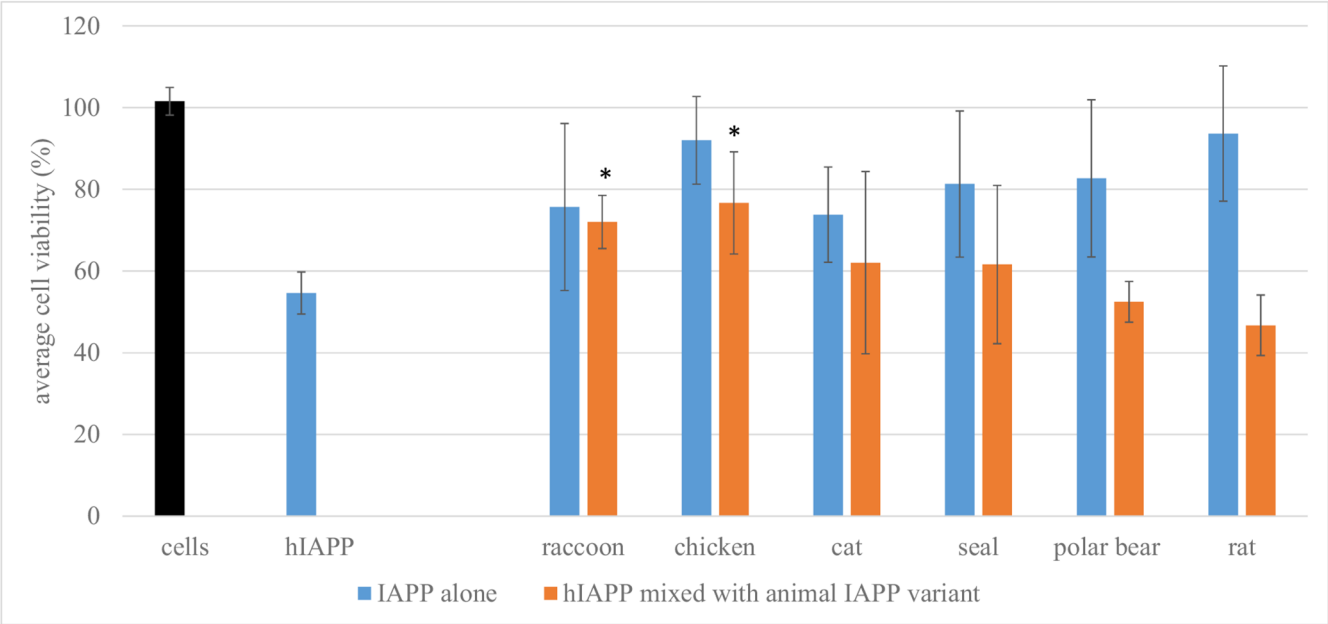

Figure 6.

MTT viability assay showing the average of four separate experiments performed in triplicate. The black bar shows the average viability of cells alone. The blue bars indicate the average cell viability upon the addition of 12.8 μM hIAPP or animal IAPP variants individually (animals indicated on the horizontal axis). The red bars display cell viability of hIAPP mixed with each animal IAPP variant (1:1 ratio of each IAPP with 12.8 μM of individual IAPP). Asterisks show a significant increase ($p<0.05$) in cell viability between hIAPP alone and hIAPP mixed with raccoon or chicken IAPP variants.

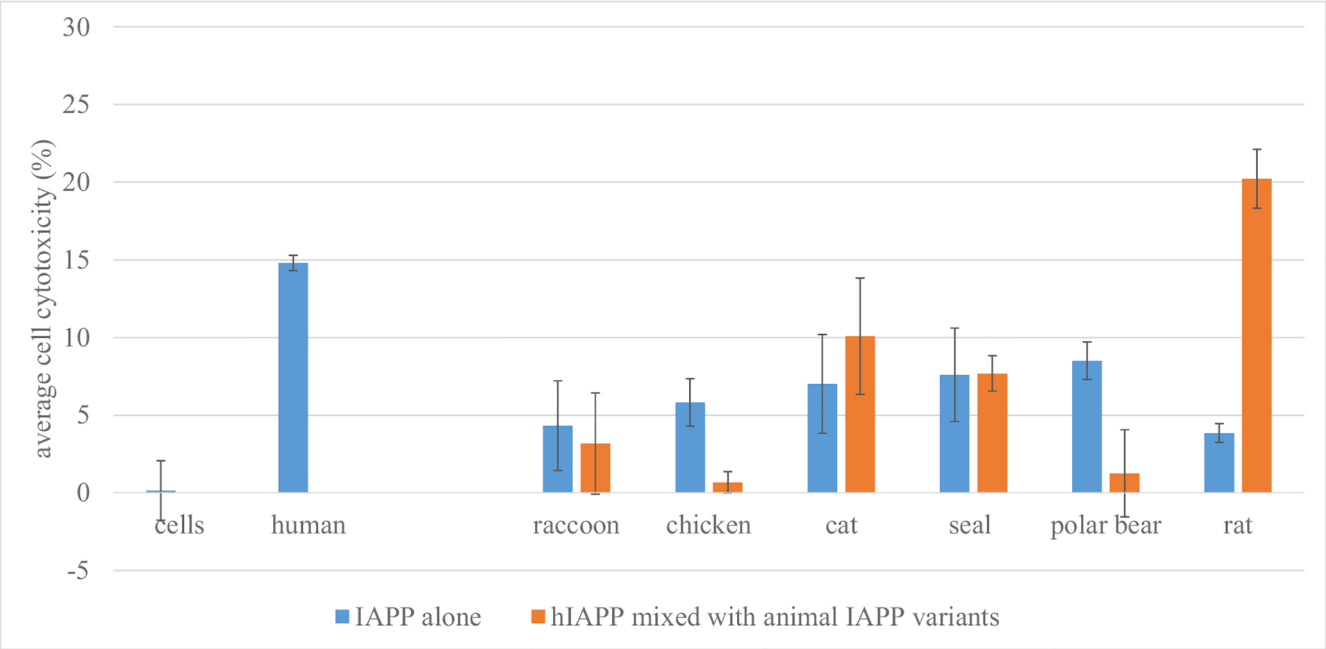

Figure 7.

LDH cytotoxicity assay. The first bar shows the average cytotoxicity of cells alone. The blue bars indicate the average cell cytotoxicity upon addition of 12.8 μM hIAPP or animal IAPP variants individually (animals indicated on the horizontal axis). The red bars display cell cytotoxicity of hIAPP mixed with each animal IAPP variant (1:1 ratio of each IAPP with 12.8 μM of individual IAPP).

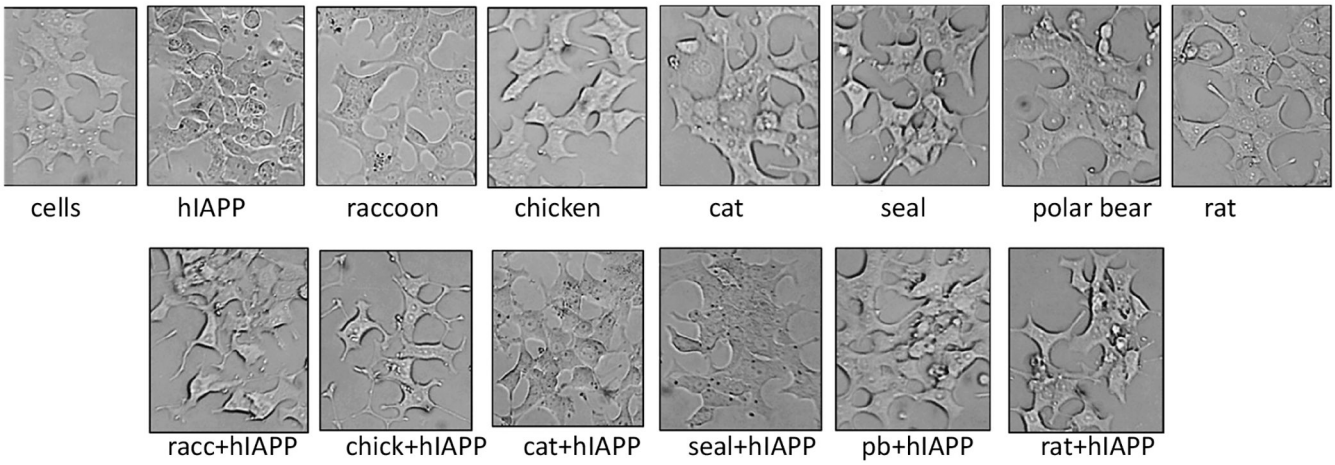

Figure 8.

Cell morphology. The top panel shows cells alone, cells treated with 12.8 μM hIAPP, and cells treated with 12.8 μM of each IAPP animal variant. The bottom panel shows cells treated with 12.8 μM of hIAPP mixed with each IAPP animal variant (1:1 ratio of each IAPP).

Table 1.

Vendor and purity of synthetic animal IAPP samples used in this study.

Organism IAPP	Company Provider	Purity
Cat	Watson BioSciences	96.0%
Chicken	Watson BioSciences	96.8%
Pig	Watson BioSciences	95.1%
Polar Bear	Watson BioSciences	96.6%
Seal	Watson BioSciences	95.9%
Raccoon	Watson BioSciences	96.4%
Raccoon	Lifetein	95.5%